



Quantum biochemistry, molecular docking, and dynamics simulation revealed synthetic peptides induced conformational changes affecting the topology of the catalytic site of SARS-CoV-2 main protease

Jackson L. Amaral^a , Jose T. A. Oliveira^a, Francisco E. S. Lopes^{a,c}, Cleverson D. T. Freitas^a, Valder N. Freire^b, Leonardo V. Abreu^a and Pedro F. N. Souza^a 

^aDepartment of Biochemistry and Molecular Biology, Federal University of Ceará, Fortaleza, Brazil; ^bDepartment of Physics, Federal University of Ceará, Fortaleza, Brazil; ^cCenter for Permanent Education in Health Care, CEATS/School of Public Health of Ceará-ESP-CE, Fortaleza, Brazil

Communicated by Ramaswamy H. Sarma

ABSTRACT

The recent outbreak caused by SARS-CoV-2 continues to threaten and take many lives all over the world. The lack of an efficient pharmacological treatments are serious problems to be faced by scientists and medical staffs worldwide. In this work, an *in silico* approach based on the combination of molecular docking, dynamics simulations, and quantum biochemistry revealed that the synthetic peptides *RcAlb*-Pepl, PepGAT, and PepKAA, strongly interact with the main protease (Mpro) a pivotal protein for SARS-CoV-2 replication. Although not binding to the proteolytic site of SARS-CoV-2 Mpro, *RcAlb*-Pepl, PepGAT, and PepKAA interact with other protein domain and allosterically altered the protease topology. Indeed, such peptide-SARS-CoV-2 Mpro complexes provoked dramatic alterations in the three-dimensional structure of Mpro leading to area and volume shrinkage of the proteolytic site, which could affect the protease activity and thus the virus replication. Based on these findings, it is suggested that *RcAlb*-Pepl, PepGAT, and PepKAA could interfere with SARS-CoV-2 Mpro role *in vivo*. Also, unlike other antiviral drugs, these peptides have no toxicity to human cells. This pioneering *in silico* investigation opens up opportunity for further *in vivo* research on these peptides, towards discovering new drugs and entirely new perspectives to treat COVID-19.

ARTICLE HISTORY

Received 30 September 2020
Accepted 16 April 2021

KEYWORDS

SARS-CoV-2 main protease;
COVID-19;
synthetic peptides

1. Introduction

The current coronavirus outbreak caused by severe acute respiratory syndrome coronavirus 2 (SARS-CoV-2) is the third epidemic event related to Coronaviruses in the last twenty years. The other two outbreaks that were caused by severe acute respiratory syndrome coronavirus 1 (SARS-CoV-1) and Middle East respiratory syndrome coronavirus (MERS-CoV) absolutely were not as severe and aggressive as SARS-CoV-2 (Song et al., 2019; WHO, 2020). To date, SARS-CoV-2 has infected 20,972,577 people in 215 countries with 750,377 deaths (CDC, n.d; Hui et al., 2020; Practice, 2020) and transmission still continues to accelerate in different geographic region of the world. Often, the main problem caused by SARS-CoV-2 in infected patients is the immune response triggered against the virus infection. This immune reaction is characterized by overproduction of the proinflammatory cytokines tumor necrosis factors (TNFs) and interleukins IL-6 and 1, known as the “cytokine storm,” which is a hyperinflammatory state that led to multiple-organ damage and

dysfunction, specially of lungs, heart, liver, and kidneys (Li et al., 2020; Ragab et al., 2020; Tang et al., 2020).

First identified in Wuhan, China, genomic data analysis revealed that the human coronavirus SARS-CoV-2 has 70% genetic similarity with SARS-CoV-1 (Almazán et al., 2014; Wu et al., 2020). One of the common features amongst these coronaviruses is that they entry in human cells by physical interaction of the viral spike glycoprotein (S protein) with the human angiotensin-converting enzyme 2 (ACE2) receptor, which is located at the cell membrane. Subsequently, conformational alteration of the S protein permits both the viral envelope to combine with the outer membrane and the transport of the virus’ genetic material inside the human cell. However, amino acid sequence data analysis showed the SARS-CoV-2S protein possesses mutations in the receptor-binding domain (RBD), in relation to that of SARS-CoV-1S protein. Such genetic alteration leads to 20-fold increased affinity of SARS-CoV-2S protein to ACE2, compared to SARS-CoV-1S protein, and enhanced infectivity and velocity of SARS-CoV-2 spreading in humans (Souza et al., 2021; Hoffmann et al., 2020; Yuan et al., 2017). Once inside the

CONTACT Jackson L. Amaral  jacksoncesarc@gmail.com  Department of Biochemistry and Molecular Biology, Federal University of Ceará, Fortaleza, CE, Brazil; Pedro F. N. Souza  pedrofilhobio@gmail.com  Laboratory of Plant Defense Proteins, P.O. Box: 60451, Av. Mister Hull, Fortaleza, CE, Brazil

 Supplemental data for this article is available online at <https://doi.org/10.1080/10426507.2020.1860983>.

target cells, SARS-CoV-2 uses its main protease (Mpro), a pivotal protein for SARS-CoV-2 replication process, across the mechanism of viral replication (Ziebuhr et al., 2000). Therefore, besides the viral spike glycoprotein (S protein), SARS-CoV-2 Mpro has taken as other potential pharmacological target for drug action against SARS-CoV-2 infection (Estrada, 2020; Hall & Ji, 2020; Ngo et al., 2020; Ortega et al., 2020).

Although SARS-CoV-2 belongs to the genus coronavirus, as SARS-CoV-1 and MERS-CoV, its infection leads to a completely novel and unknown disease, coronavirus disease 2019 (COVID-19), which is ending human life and taking over the economy globally (Saxena, 2020). Indubitable, there is an urgent need to discover and develop effective drugs to combat the virus and discontinue the disastrous consequences it has brought to mankind. To speed up novel drug discovery and development for COVID-19 treatment, the integrated use of bioinformatics approaches, such as molecular docking, dynamics simulations, and quantum analysis (Liu et al., 2020; Morais et al., 2020; Ngo et al., 2020) allows to select potential antiviral molecules to be subsequently tested *in vitro* and *in vivo* against SARS-CoV-2 and other viruses.

Recently, our research group, by using bioinformatics approaches, found out that the synthetic peptides Mo-CBP3-PepII and PepKAA targeted SARS-CoV-2 spike protein and induced conformational alterations that disrupt its correct binding to the ACE2 receptor (Souza et al., 2020). In this current study, which was conducted to further exploit the peptide-based therapeutic approach to treat COVID-19, the integrated use of these above mentioned bioinformatics methods was employed to assess whether any out of the following eight synthetic small peptides, Mo-CBP₃-PepI, Mo-CBP₃-PepII, Mo-CBP₃-PepIII (Oliveira et al., 2019), RcAlb-PepI, RcAlb-PepII, RcAlb-PepIII (Dias et al., 2020), PepGAT, and PepKAA (Souza et al., 2020), which were designed based on plant proteins purified by our research group, could physically interact with SARS-CoV-2 Mpro and inhibit both its binding to ACE2 cell membrane receptor and its crucial activity. Briefly, amongst the tested peptides, RcAlb-PepI, PepGAT, and, particularly, PepKAA interact with SARS-CoV-2 Mpro at a region far away from the active site, but induce conformational alterations of the protease that promote shrinkage of its catalytic domain. These results suggest that RcAlb-PepI, PepGAT, and PepKAA could allosterically inhibit the SARS-CoV-2 Mpro activity and theoretically prevent viral replication and, consequently, *spread* of SARS-CoV-2 infection. Certainly, this hypothesis must be tested *in vitro* before being tested *in vivo*.

2. Methodology

2.1. Three-dimensional structures

The three-dimensional (3D) structures of Mo-CBP₃-PepI, Mo-CBP₃-PepII, and Mo-CBP₃-PepIII were identical to those used by Oliveira et al. (2019). The 3D structures of RcAlb-PepI, RcAlb-PepII, and RcAlb-PepIII were equal to those employed by Dias et al. (2020). The PepGAT and PepKAA 3D structures were identical to those used by Souza et al. (2020). The 3D

structure files of SARS-CoV-2 main protease (Mpro) (PDB: 6M03) were downloaded from Protein Data Bank (PDB, <https://www.rcsb.org/>).

2.2. Molecular docking assays

Blind molecular docking analyses were carried out in FRODOCK 3.12 (Ramírez-Aportela et al., 2016) and ClusPro 2.0 (<https://cluspro.org>), using the synthetic peptides as ligands against SARS-CoV-2 Mpro. Docking scores were used to select the peptides with the highest potential for interaction with SARS-CoV-2 Mpro. A score of 1 was assigned to the peptide with the highest docking value (referred to as the top scored pose). The scores of the subsequent peptides were decreased successively by a factor of 0.125 as the docking values decreased in relation to that of the peptide that received score 1. The peptide score obtained in the FRODOCK was added to that generated by ClusPro. Based on the sum of scores, the three peptides with the highest potential were used to conduct the subsequent studies.

2.3. Molecular dynamics simulation

To stabilize the complexes formed between SARS-CoV-2 Mpro and the studied peptides before molecular dynamics simulation using Gromacs version 2018.4 (Van Der Spoel et al., 2005), they were minimized and equilibrated. OPLS-AA/L all-atom force field (Moal & Bates, 2010; Robertson et al., 2015) was used to build molecular topology. Then, a cubic water box of edge length 2 nm was created. Box solvation was done with the SPC/E water model, the systems were neutralized, and Na⁺ and Cl⁻ added at 0.15 M concentration. Energy minimization of the complex structure was carried out until a negative potential energy and a maximum force below 10³ kJ mol⁻¹ nm⁻¹ were attained. Next, temperature and pressure equilibration were performed during 100 ps simulation. Molecular dynamics simulations, in duplicate, were performed during 100 ns and the final structures generated were used for further analysis.

2.4. Interface analysis of the complexes formed between SARS-CoV-2 Mpro and the studied peptides

This analysis was carried out using the Protein Interactions Calculator (PIC) webserver (<http://pic.mbu.iisc.ernet.in/>). The 2D figures showing hydrogen bonds and hydrophobic interactions were built using the Ligplot software (Laskowski & Swindells, 2011). The Pymol software was used to generate 3D structures and to calculate RMSD (root mean square deviation) (Laskowski et al., 2018). CASTp 3.0 (Tian et al., 2018) was used to assess changes in the area and volume of the proteolytic site of the SARS-CoV-2 main protease (SARS-CoV-2 M'pro) when alone and complexed with the studied peptides.

Table 1. Molecular docking parameters of the interactions between the studied synthetic peptides and SARS-CoV-2 Mpro.

Peptide	FRODOCK ^a	Punctuation ^b	ClusPro ^c	Punctuation ^d	Sum ^e
Mo-CBP3-Pepl	1816.15	0.375	-603.5	0.250	0.625
Mo-CBP3-Pepll	1809.39	0.250	-736.5	1.000	1.250
Mo-CBP3-Peplll	1700.10	0.125	-654.0	0.625	0.750
RcAlb-Pepl	2021.32	0.750	-579.1	0.125	0.875
RcAlb-Pepll	2002.75	0.625	-694.5	0.875	1.500
RcAlb-Peplll	1871.59	0.500	-654.7	0.750	1.250
PepGAT	2061.69	0.875	-642.2	0.500	1.375
PepKAA	2182.11	1.000	-632.7	0.375	1.375

^aCalculated using the FRODOCK v.3.12 server.

^{b,d}Punctuation is associated with both the FRODOCK score and the ClusPro lowest binding free energy (kcal mol⁻¹), respectively. A score of 1 was assigned to the peptide with the highest docking value (referred to as the top scored pose). The scores of the subsequent peptides were decreased successively by a factor of 0.125 as the docking values decreased in relation to that of the peptide that received score 1.

^cThe lowest binding free energy (ΔG) calculated using ClusPro 2.0.

^eRepresents the sum of the scores (punctuation) in b and d.

2.5. Quantum biochemistry calculation

This was performed according to a protocol established previously by Zhang and Zhang (2003). Molecular fractionation with conjugate caps (MFCC) was carry out to calculate *in silico* the full quantum mechanical interaction energies between two pairs of specific amino acid residues (Ri and Rj) involving the studied peptides and SARS-CoV-2 Mpro, as follows, based on the work of Amaral et al. (2020):

$$E(R_i - R_j) = E(C_{i-1}R_iC_{i+1} + C_{j-1}R_jC_{j+1}) - E(C_{i-1}R_iC_{i+1} + C_{j-1}C_{j+1}) - E(C_{i-1}C_{i+1} + C_{j-1}R_jC_{j+1}) + E(C_{i-1}C_{i+1} + C_{j-1}C_{j+1})$$

Where $E(C_{i-1} R_i C_{i+1} + C_{j-1} R_j C_{j+1})$, the first term of the equation, is the total energy of the system formed by the residues Ri and Rj correctly capped; $E(C_{i-1} R_i C_{i+1} + C_{j-1} C_{j+1})$, the second term, is the total energy of the system formed by the capped residue Ri and the caps of the residue Rj; the third term, $E(C_{i-1} C_{i+1} + C_{j-1} R_j C_{j+1})$, represents the total energy of the system formed by the capped residue Rj and the caps of the residue Ri; and the last term, $E(C_{i-1} C_{i+1} + C_{j-1} C_{j+1})$, accounts for the total energy of the system formed by the caps of both residues Ri and Rj. The caps $C_{i-1}(C_{i+1})$ and $C_{j-1}(C_{j+1})$ are made from the residues covalently bound to the amine (carboxyl) groups of Ri and Rj. In the MFCC method used, all interaction between amino acid residues of the studied peptides and SARS-CoV-2 Mpro separated from each other within a 8 Å range were calculated, considering a dielectric function approaches of 40 ($\epsilon = 40$) for all interactions. The structural files (PDB format) obtained after molecular dynamics simulation and MFCC were used as inputs for density functional theory calculations with DMOL³ (Delley, 2000).

3. Results

3.1. Molecular docking parameters of the interaction between the synthetic peptides and SARS-CoV-2 Mpro

Before molecular dynamics and quantum biochemistry analyses, molecular docking simulations were run on the FRODOCK 3.12 and ClusPro 2.0 web servers to find out which

peptides best interact with SARS-CoV-2 Mpro. Both servers calculated that the eight studied peptides bind strongly to SARS-CoV-2 Mpro with score values that varied from 1700.10 to 2182.11 (Table 1). ClusPro 2.0 was used to calculate the free energies (ΔG) of interactions, which were low and varied from -579.1 to -736.5 kcal.mol⁻¹ (Table 1). The sum of the punctuations provided by FRODOCK and ClusPro 2.0 was used to select RcAlb-pepll, PepGAT, and PepKAA as the best peptides, in relation to their capacity of binding to SARS-CoV-2 Mpro, with punctuation values of 1.500, 1.375, and 1.375, respectively (Table 1). Molecular docking analysis also revealed that these peptides do not bind to the proteolytic site of SARS-CoV-2 Mpro (His⁴¹ and Cys¹⁴⁵) (Figure 1). Nevertheless, RcAlb-pepll, PepGAT, and PepKAA were further analyzed using molecular dynamics and quantum biochemistry.

3.2. Molecular dynamics simulation

Molecular dynamics simulations were done with SARS-CoV-2 Mpro alone and complexed with the peptides RcAlb-pepll, PepGAT, and PepKAA. RMSD of SARS-CoV-2 Mpro alone and complexed with the peptides increased gradually up to 1.5 Å within 50 ns and then remained stable until 100 ns, with RMSD fluctuation below 1 Å (Figure 2). The stable conformation obtained from each molecular dynamics simulation was used to perform further analyzes.

3.3. Interaction between SARS-CoV-2 Mpro with RcAlb-Pepll

The key amino acid residues responsible for the multi-point binding interactions between SARS-CoV-2 Mpro and RcAlb-Pepll were Lys¹³⁷, Asn²⁷⁴, Met²⁷⁶, Tyr²³⁷, and Asn²⁷⁷ with Leu⁹, Lys², Lys², Pro⁵, and Lys² (Table 2; Figure 3A, B and D) with interaction energy of -12.13, -8.30, -4.82, -4.60, and -3.75 kcal.mol⁻¹, respectively (Table 2). Repulsive interactions occur between the amino acid residues Asp¹⁹⁷, Lys¹³⁷, and Glu²⁹⁰ of SARS-CoV-2 Mpro with Leu⁹, Ala⁸, and Leu⁹ of RcAlb-Pepll, with interaction energy of +1.64, +1.66, and +1.92 kcal mol⁻¹ and distance of 1.64, 1.66, and 1.92 Å, respectively (Table 2). Supplementary Table 1 shows the quantum parameters of the multi-point binding interactions between the amino acid residues of SARS-CoV-2 Mpro and those of RcAlb-Pepll at distances up to 8 Å. The complex formed between SARS-CoV-2 Mpro and RcAlb-Pepll is molded through hydrophobic interactions established by the amino acid residues Tyr²³⁷, Tyr²³⁹, Tyr²³⁹, Leu²⁷¹, Leu²⁷², Leu²⁷², Met²⁷⁶, Leu²⁸⁶, Leu²⁸⁶, Leu²⁸⁶, Leu²⁸⁷, and Leu²⁸⁷ of SARS-CoV-2 Mpro with Pro⁵, Ile⁴, Leu⁹, Ile⁴, Ile⁴, Pro⁵, Ile⁴, Ile⁴, Ile⁷, Leu⁹, Ile⁴, and Leu⁹ of RcAlb-Pepll (Figure 3A, B and D). Hydrogen bonds are established between the amino acid residues Met²⁷⁶ and Asn²⁷⁴ of SARS-CoV-2 Mpro with Lys² of RcAlb-Pepll (Figure 3A, B and D). The individual interaction energy of the residues Ala¹, Lys², Leu³, Ile⁴, Pro⁵, Thr⁶, Ile⁷, Ala⁸, Leu⁹ was -5.28, -20.44, -3.55, -10.60, -5.86, -0.74, -11.58, -5.98, and -10.83 kcal.mol⁻¹, respectively (Figure 3C).

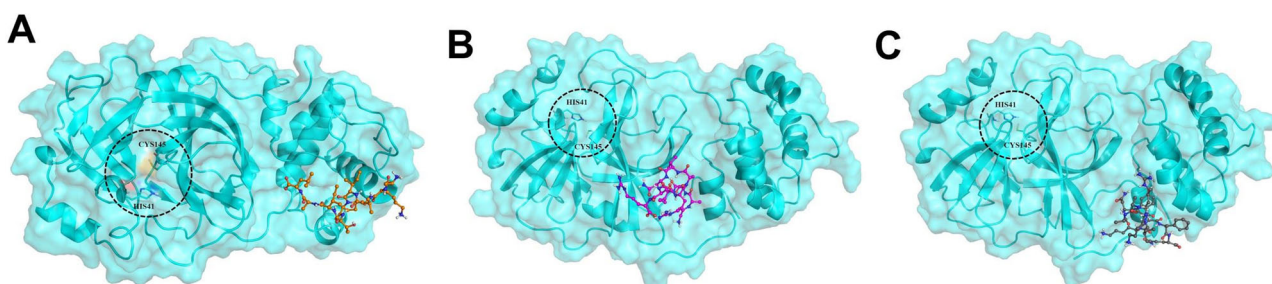


Figure 1. Complexes formed by docking of the peptides RcAlb-Pepl1 (A), PepGAT (B), and PepKAA (C) on SARS-CoV-2 Mpro.

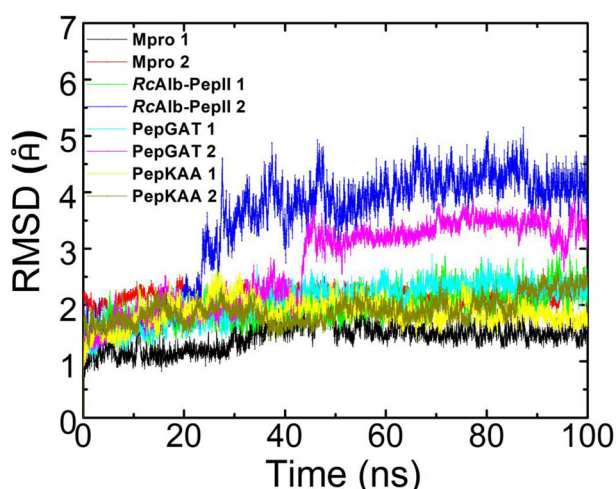


Figure 2. RMSD plot of the conformation stability of SARS-CoV-2 Mpro alone and of the complexes formed by docking of RcAlb-Pepl1, PepGAT, and PepKAA on SARS-CoV-2 Mpro as a function of time (ns).

3.4. Interaction between SARS-CoV-2 Mpro with PepGAT

Distances (Å), total free energy of interaction (kcal mol^{-1}), amino acid residue charge and amino acid residue atom closest (up to 8 Å) to the interactions between SARS-CoV-2 Mpro and PepGAT are shown in the [supplementary Table 2](#). Interaction between SARS-CoV-2 Mpro and PepGAT was established predominantly by Gln³⁰⁶, Asp¹⁵³, Asp²⁴⁸, Phe²⁹⁴, Gln¹¹⁰, Ile²⁴⁹, Phe²⁹⁴, and Asp²⁴⁵ with Gly¹, Arg⁵, Gly¹, Arg¹⁰, Arg⁵, Thr³, Arg¹⁰, Ala², and Arg¹⁰, with interaction energy of -19.62 , -12.35 , -11.12 , -10.39 , -6.28 , -4.73 , -4.51 , -3.96 , and $-3.89 \text{ kcal.mol}^{-1}$, and distances of 1.57, 2.32, 2.50, 2.80, 2.31, 2.23, 2.10, 4.12, and 2.54 Å, respectively, to form stable complex ([Table 3](#); [Figure 4A and B](#)). Repulsive interactions occur mainly between the amino acid residues Arg²⁹⁸, Lys¹⁰², and Phe³⁰⁵ of the protease with Gly¹ of the peptide, with interaction energy of $+1.47$, $+2.26$, and $+2.79 \text{ kcal.mol}^{-1}$ and distances of 6.14, 5.39, and 3.49 Å, respectively ([Table 3](#)).

[Supplementary Table 2](#) shows the quantum parameters of the multi-point binding interactions between the amino acid residues of SARS-CoV-2 Mpro and those of PepGAT at distances up to 8 Å. SARS-CoV-2 Mpro establishes hydrophobic, ionic, cation-pi and hydrogen bond interactions with PepGAT. Hydrogen bonds are established between the amino acid residues Gln¹¹⁰, Asp¹⁵³, and Asp²⁴⁸ of SARS-CoV-2 Mpro with Thr³, Gly¹, and Arg¹⁰ of PepGAT ([Figure 4A, B, and D](#)). The ionic interactions occur between the amino acid residues Asp²⁴⁵ and Asp²⁴⁸ of Mpro with Arg¹⁰ of PepGAT

([Figure 4A, B and D](#)). A cation-pi interaction is formed by Phe²⁹⁴ of SARS-CoV-2 Mpro with Arg¹⁰ of PepGAT. Hydrophobic interactions are established by the amino acid residues Val¹⁰⁴, Ile²⁴⁹, Phe²⁹⁴, and Phe²⁹⁴ of SARS-CoV-2 Mpro with Ile⁴, Ala⁶, Ala², and Ala⁶ of PepGAT ([Figure 4B and D](#)). The individual interaction energy of the residues Gly¹, Ala², Thr³, Ile⁴, Arg⁵, Ala⁶, Val⁷, Asn⁸, Ser⁹, and Arg¹⁰ of PepGAT was -19.73 , -6.59 , -12.20 , -12.10 , -16.45 , -3.56 , -6.26 , -0.80 , -0.74 , and $-22.80 \text{ kcal.mol}^{-1}$, respectively ([Figure 4C](#)).

3.5. Interaction between SARS-CoV-2 Mpro with PepKAA

The key amino acid residues responsible for the multi-point binding interactions between SARS-CoV-2 Mpro and PepKAA are Asp²⁴⁵, Asp²⁴⁸, Asp²⁴⁸, Gln²⁵⁶, Phe²⁹⁴, Asp¹⁵³, Ile²⁴⁹, Pro²⁵², and Val²⁹⁷ with Arg⁵, Arg⁵, Lys¹, Phe⁹, Tyr⁸, Lys⁷, Arg⁵, Tyr⁸, and Tyr⁸ with interaction energy of -11.93 , -11.32 , -10.36 , -6.55 , -6.08 , -4.93 , -4.03 , -3.60 , and $-3.29 \text{ kcal.mol}^{-1}$ and distances of 1.68, 1.76, 3.71, 2.70, 2.31, 3.79, 2.60, 2.14, and 2.14 Å, respectively ([Table 4](#)). The repulsive interactions occur between Val²⁴⁷ and Lys¹⁰² of SARS-CoV-2 Mpro with Arg⁵ and Lys⁷ of PepKAA, with interaction energy of $+0.58$ and $+1.34 \text{ kcal.mol}^{-1}$ and distances of 6.08 and 7.05 Å, respectively ([Table 4](#)). [Supplementary Table 3](#) shows the quantum parameters of the multi-point binding interactions between the amino acid residues of SARS-CoV-2 Mpro and those of PepKAA at distances up to 8 Å. SARS-CoV-2 Mpro binds to PepKAA through hydrophobic, ionic, aromatic, and hydrogen bond interactions. Hydrogen bonds are formed by Asp²⁴⁵ and Asp²⁴⁸ of SARS-CoV-2 Mpro with Arg⁵ of PepKAA ([Figure 5A, B and D](#)). Ionic interactions occur between Asp¹⁵³, Asp²⁴⁵, Asp²⁴⁸, and Asp²⁴⁸ of SARS-CoV-2 Mpro with Lys⁷, Arg⁵, Lys¹, and Arg⁵ of PepKAA, respectively ([Figure 5B and D](#)). Hydrophobic interactions are established by Ile²¹³, Pro²⁵², Pro²⁵², Pro²⁵², Leu²⁵³, Leu²⁵³, Pro²⁹³, Phe²⁹⁴, Val²⁹⁶, and Val²⁹⁷ of SARS-CoV-2 Mpro with Phe⁹, Ile⁶, Tyr⁸, Phe⁹, Tyr⁸, Phe⁹, Tyr⁸, Tyr⁸, Phe⁹, and Tyr⁸ of PepKAA. An aromatic interaction is formed by Phe²⁹⁴ of SARS-CoV-2 Mpro with Tyr⁸ of PepKAA ([Figure 5A and D](#)). The individual interaction energy of the residues Lys¹, Ala², Ala³, Asn⁴, Arg⁵, Ile⁶, Lys⁷, Tyr⁸, Phe⁹, Gln¹⁰ of PepKAA was -6.27 , -1.06 , $+0.05$, -0.80 , -25.54 , -2.34 , -11.91 , -22.90 , -13.16 , and $-8.42 \text{ kcal.mol}^{-1}$, respectively ([Figure 5C](#)).

Table 2. Quantum parameters of the multi-point binding interactions between the amino acid residues of SARS-CoV-2 Mpro and those of *RcAlb*-PepII.

Amino acid residues		Distance (Å)		Free energy of interaction (kcal mol ⁻¹)		Residue charge		Residue atom	
SARS-CoV-2 Mpro	<i>RcAlb</i> -PepII	SARS-CoV-2 Mpro	<i>RcAlb</i> -PepII	SARS-CoV-2 Mpro	<i>RcAlb</i> -PepII	SARS-CoV-2 Mpro	<i>RcAlb</i> -PepII	SARS-CoV-2 Mpro	<i>RcAlb</i> -PepII
LYS137	LEU9	1.80	-12.13	1	-1	1	-1	HZ3	O2
ASN274	LYS2	2.79	-8.30	0	1	0	1	O	HZ1
MET276	LYS2	2.17	-4.82	0	1	0	1	H	O
TYR237	PRO5	2.57	-4.60	0	0	0	0	CE1	HG1
ASN277	LYS2	2.39	-3.75	0	1	0	1	OD1	HD2
LEU287	ILE4	2.33	-2.99	0	0	0	0	HD13	HD1
LEU287	LEU9	2.33	-2.86	0	-1	0	-1	HB2	HD11
LEU286	LEU9	2.42	-2.82	0	-1	0	-1	HD12	HB2
LEU272	ILE4	2.44	-2.77	0	0	0	0	HA	HB
GLY275	LYS2	2.44	-2.75	0	1	0	1	HA1	O
LEU286	ILE7	2.82	-2.75	0	0	0	0	HD21	HG22
LEU272	PRO5	2.50	-2.63	0	0	0	0	HA	HD2
ARG131	LEU9	5.02	-2.08	1	-1	1	-1	HH12	O1
THR199	LEU9	2.63	-1.94	0	-1	0	-1	HG23	HD12
LEU271	ILE4	2.68	-1.88	0	0	0	0	HB2	HG12
ASP197	LEU9	6.44	1.64	-1	-1	-1	-1	OD1	O2
LYS137	ALA8	5.44	1.66	1	0	1	0	HZ3	C
GLU290	LEU9	5.70	1.92	-1	-1	-1	-1	OE2	O1

3.6. Quantum biochemistry description

The most important amino acid residues of SARS-CoV-2 Mpro that interact with *RcAlb*-PepII are Leu²⁸⁷, Leu²⁸⁶, Asn²⁷⁴, Gly²⁷⁵, Met²⁷⁶, Lys¹³⁷, Tyr²³⁷, Leu²⁷², and Asn²⁷⁷ with interaction energy of -9.36, -9.03, -8.78, -6.47, -6.46, -6.41, -5.97, -5.80, and -5.60 kcal.mol⁻¹, respectively. The Asp¹⁹⁷, Asp²⁸⁹, and Glu²⁹⁰ residues showed repulsive energies (Figure 6A). The sum of all free energies of interaction between SARS-CoV-2 Mpro and *RcAlb*-PepII (Et) was -74.85 kcal.mol⁻¹ (Figure 7).

The key amino acid residues involved in the interaction of SARS-CoV-2 Mpro with the PepGAT are Asp¹⁵³, Gln³⁰⁶, Phe²⁹⁴, Asp²⁴⁸, and Asp²⁴⁵ with interaction energy of -12.47, -11.27, -8.36, -6.67, and -4.72 kcal.mol⁻¹, respectively. Residues of Arg²⁹⁸, Phe³⁰⁵, Lys¹⁰² showed small repulsive energies (Figure 6B). The sum of all free energies of interaction between SARS-CoV-2 Mpro with PepGAT was -101.2 kcal.mol⁻¹ (Figure 7).

The major amino acid residues of the interaction between SARS-CoV-2 Mpro and PepKAA are Asp²⁴⁸, Pro²⁵², Phe²⁹⁴, Asp¹⁵³, and Asp²⁴⁵, with interaction energy of -20.14, -11.27, -10.15, -9.57, and -8.17 kcal. mol⁻¹, respectively. Lys¹⁰² showed a small repulsive energy (Figure 6C). The sum of all free energies of interaction between SARS-CoV-2 Mpro and PepKAA was -92.35 kcal.mol⁻¹ (Figure 7).

3.7. Assessment of the conformational changes induced by *RcAlb*-PepII, PepGAT, and PepKAA in the area and volume of the proteolytic site of SARS-CoV-2 Mpro

RMSD analyses revealed that *RcAlb*-PepII, PepGAT, and PepKAA induced alterations in the 3D structure of SARS-CoV-2 Mpro (Figure 8). The control structure presented RMSD value of 0, which indicates a typical and functional 3D structure (Figure 8A). However, the structural alignment of SARS-CoV-2 Mpro complexed with *RcAlb*-PepII, PepGAT, or PepKAA revealed several alterations in the SARS-CoV-2 Mpro

structure, which was confirmed by the RMSD values of 3.118, 3.164, 3.054 Å, respectively (Figure 8B-D).

These structural changes in SARS-CoV-2 Mpro induced by interactions with the studied peptides lead to alterations in the area and volume of the SARS-CoV-2 Mpro proteolytic site. SARS-CoV-2 Mpro itself, not complexed with the studied peptides, presented an area and volume of 279.7 Å² and 298.1 Å³, respectively (Figure 9A).

When complexed with *RcAlb*-PepII, the area and volume of SARS-CoV-2 Mpro proteolytic site reduced to 120.6 Å² and 93.3 Å³, which represent 68.7% and 56.9% decrease, respectively (Figure 9B). The structural changes caused by PepGAT also reflected in the area and volume of the SARS-CoV-2 Mpro proteolytic site, which decreased from 298.1 Å² and 279.7 Å³ to 183.7 Å² and 179.0 Å³, resulting in a 38.4% and 36.0% decrease, respectively (Figure 9C). Regarding to PepKAA, its interaction with the protease promoted a 13.0% (279.7 Å² to 243.3 Å²) and 23.1% (298.1 Å³ to 229.2 Å³) decrease, respectively, in the area and volume of the SARS-CoV-2 Mpro proteolytic site (Figure 9D).

4. Discussion

Currently, there are two main ways to find out and develop medicines against SARS-CoV-2. The first one is through drug repositioning in which the antiviral activity of several pharmacological classes of medicines already approved for use in humans is investigated as a possibility for generating new treatments against COVID-19 (Diamond & Pierson, 2020; Serafin et al., 2020; Tay et al., 2020; Zhang et al., 2020). To date, such attempts have been tried unsuccessfully. The second approach is still a promise, but it is based on systematic investigations conducted to identify novel small molecules designed to target key SARS-CoV-2 factors such as the Spike glycoprotein and RNA polymerase (Souza et al., 2020). Such an approach involves the *in silico* molecular docking and molecular dynamics simulation, which are structure-based method employed to predict the binding affinity of a

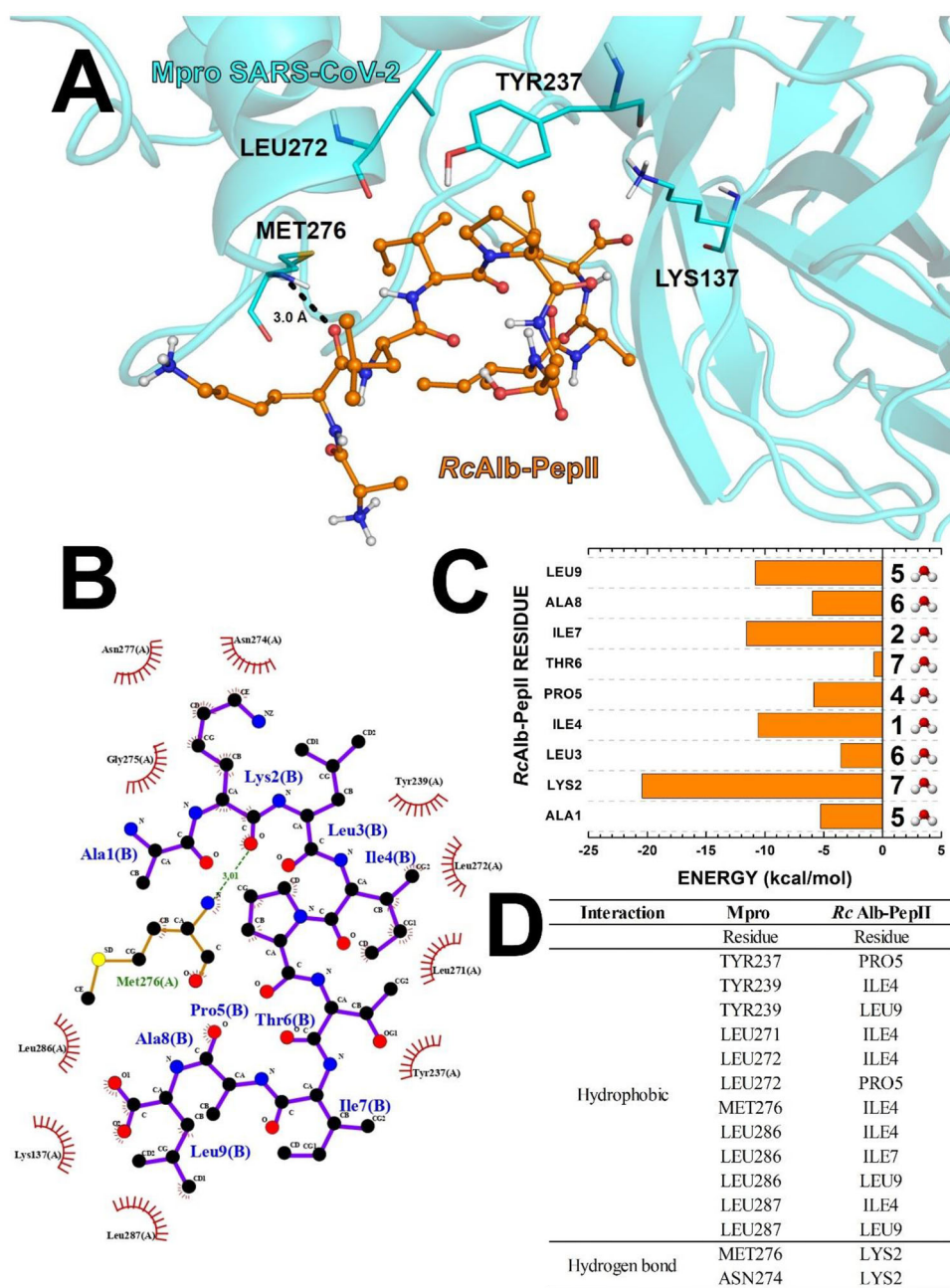


Figure 3. The 3D and 2D structure representations of the complex formed by docking of *RcAlb-PepII* (Ala¹-Lys-Leu-Ile-Pro-Thr-Ile-Ala-Leu⁹) on SARS-CoV-2 Mpro are depicted in A and B, respectively. The interaction energies of the amino acid residues of *RcAlb-PepII* with those of SARS-CoV-2 Mpro, and the amino acid residues that participate in the hydrophobic interactions and hydrogen bonds between *RcAlb-PepII* and SARS-CoV-2 Mpro are shown in C and D, respectively.

ligand molecule to a target (Dai et al., 2020; Hall & Ji, 2020; Ngo et al., 2020; Ortega et al., 2020; Zhang et al., 2020).

So, molecular docking and molecular dynamics simulation constitute useful tools to facilitate the drug development process as they allow to predict *in silico* the binding affinity of a designed ligand molecule to a target as SARS-CoV-2 Mpro (Zhang et al., 2020). Mpro has three-domain (domains I to III) cysteine protease essential for coronavirus replication as it plays a crucial role in the processing of the viral polyproteins into mature proteins (Ziebuhr et al., 2000). SARS-CoV-2 Mpro and SARS-CoV-1 Mpro primary structures differ by only 12 amino acid residues, which means they have 96% similarity (Estrada, 2020). However, a considerable difference between the catalytic site of SARS-CoV-1 and that of SARS-

CoV-2 is observed. In SARS-CoV-1 Mpro, the active site cavity is a well-defined pocket with the area and volume of 256.8 Å² and 191.24 Å³, respectively, compared to 352.1 Å² and 323.73 Å³ of that of SARS-CoV-2 Mpro (Ortega et al., 2020). These differences increase by 15% the proteolytic effectiveness of SARS-CoV-2 Mpro compared to that of SARS-CoV-1 Mpro (Estrada, 2020; Ortega et al., 2020; Zhang et al., 2020). Such higher catalytic efficiency of SARS-CoV-2 Mpro could enhance the virus replication process and formation of new virus particles, which could lead to higher infectivity. Therefore, due to its crucial involvement in maturation of most of the nonstructural proteins that are translated from SARS-CoV-2 RNA, SARS-CoV-2 Mpro is an attractive target to design antiviral drugs (Sharma et al., 2020).

Table 3. Quantum parameters of the multi-point binding interactions between the amino acid residues of SARS-CoV-2 Mpro and those of PepGAT.

Amino acid residues		Distance (Å)	Free energy of interaction (kcal mol ⁻¹)	Residue charge		Residue atom	
SARS-CoV-2 Mpro	PepGAT			SARS-CoV-2 Mpro	PepGAT	SARS-CoV-2 Mpro	PepGAT
GLN306	GLY1	1.57	-19.62	-1	1	O1	H3
GLN306	ARG5	2.32	-12.35	-1	1	O1	HH21
ASP153	GLY1	2.50	-11.12	-1	1	OD2	H2
ASP248	ARG10	2.80	-10.39	-1	0	OD1	HH12
PHE294	ARG5	2.31	-6.28	0	1	HD1	HD1
GLN110	THR3	2.23	-4.73	0	0	HE22	O
ILE249	ARG10	2.10	-4.51	0	0	HG21	HH22
PHE294	ALA2	4.12	-3.96	0	0	HB1	O
ASP245	ARG10	2.54	-3.89	-1	0	OD1	HH22
PHE294	ARG10	3.02	-2.94	0	0	HE1	HG2
GLN107	VAL7	2.76	-2.32	0	0	HG2	HG11
ILE106	THR3	2.86	-2.15	0	0	HG21	HB
ASP295	ALA2	2.41	-2.05	-1	0	HB1	HB2
ASP295	GLY1	1.92	-1.87	-1	1	HB1	C
PHE294	ALA6	2.92	-1.87	0	0	HE2	HA
ILE249	ALA6	3.83	-1.82	0	0	HG21	HA
GLN107	ALA6	6.92	-1.79	0	0	OE1	HB1
ARG298	GLY1	6.14	1.47	1	1	HD2	HA1
LYS102	GLY1	5.39	2.26	1	1	HZ3	H2
PHE305	GLY1	3.49	2.79	0	1	HD2	HA1

Many studies have tried to either analyze new drugs or already known drugs that could interact with the catalytic site of SARS-CoV-2 Mpro and inhibit its activity (Hall & Ji, 2020; Ngo et al., 2020; Ortega et al., 2020; Sharma et al., 2020; Zhang et al., 2020). Moreover, drugs that have been employed to treat HIV by inhibiting the viral protease were also tested (Hall & Ji, 2020). In this current *in silico* study we used molecular docking and dynamics simulations to predict and show that the synthetic peptides *RcAlb-PepII*, PepGAT, and PepKAA, out of eight peptides tested, interact most efficiently with SARS-CoV-2 Mpro (Table 1, Figures 1–7). These peptides interact with SARS-CoV-2 Mpro at a region far away from the protease catalytic site, which suggests that the peptides may modulate the SARS-CoV-2 Mpro activity allosterically (Figures 8 and 9). Actually, this is a pioneer study in which quantum biochemistry is employed to analyze the interaction of peptides against SARS-CoV-2 Mpro (Tables 2–4). Quantum biochemistry calculations (Morais et al., 2020; Sousa et al., 2016) allowed to deduce the individual energies of interactions of each amino acid residue of the studied peptides and those of SARS-CoV-2 Mpro. Therefore, it was possible to predict the hydrogen bonds, ionic, aromatic, and hydrophobic interactions that are important to establish attractive or repulsive interactions between the peptides and SARS-CoV-2 Mpro (Figures 3–6). Figure 7 shows that, by using quantum biochemistry calculations, the total interaction energy between *RcAlb-PepII*, PepGAT, and PepKAA with SARS-CoV-2 Mpro was -74.85 , -101.2 , and -92.35 kcal.mol⁻¹, respectively. As this is the first work that analyzes, through quantum biochemistry, interactions of peptides with SARS-CoV-2 Mpro, the results presented herein are compared with those reported by Campos et al. (2020), in which the interaction of two peptides against the Zika virus protease was analyzed. The authors demonstrated, by quantum biochemistry, that the interaction energies of the peptides *cn-716* and *acyl-KR-aldehyde* with the protease

NS2B-NS3 were -63.35 kcal.mol⁻¹ and -71.4 kcal.mol⁻¹, respectively. For instance, *RcAlb-PepII*, PepGAT, and PepKAA interacts with SARS-CoV-2 Mpro even more strongly than *cn-716* and *acyl-KR-aldehyde* to the protease *NS2B-NS3*. Nevertheless, interaction of other non-peptide-like antiviral drugs have been tested with the same purpose of inhibiting the proteolytic activity of SARS-CoV-2 Mpro. For example, Ortega et al. (2020) tested by molecular docking the interaction of the clinically proven anti-HIV drugs Saquinavir, Lopinavir, and Tripranavir, which act as inhibitors of the HIV protease, with the proteolytic site of SARS-CoV-2 Mpro. Additionally, Hall and Ji (2020) reported that Remdesivir, a nucleotide analogue initially developed to treat hepatitis C and later *Ebola* and *Marburg virus*, also binds to the proteolytic site of SARS-CoV-2 Mpro. These two later studies are referred as drug reposition or drug repurposing, which is an approach to speed up the drug discovery process through identification of a novel clinical use for an existing drug approved for a different indication (Serafin et al., 2020). Moreover, Ngo et al. (2020) docked some natural compounds and found that cannabisin A and isoacteoside interacted with the proteolytic site of SARS-CoV-2 Mpro. Currently, the most reliable inhibitor of SARS-CoV-2 Mpro, as seen by molecular docking and proven *in vitro*, is 13b, an α -ketoamide that is a protease inhibitor of coronavirus that strongly binds to the proteolytic site of SARS-CoV-2 Mpro (Zhang et al., 2020). *RcAlb-PepII*, PepGAT, and PepKAA interact with SARS-CoV-2 Mpro at a region far away from the protease active site (Figures 1, 8, and 9), contrary to these above-mentioned antiviral drugs tested. However, Bzówka et al. (2020) showed that the proteolytic site of SARS-CoV-2 Mpro has high flexibility and plasticity, which means it is highly susceptible to genetic mutational change. Such possibility constitutes a serious problem for designing drugs targeting the proteolytic site because a simple genetic mutation could prevent the action of these antiviral drugs. Actually, SARS-CoV-2

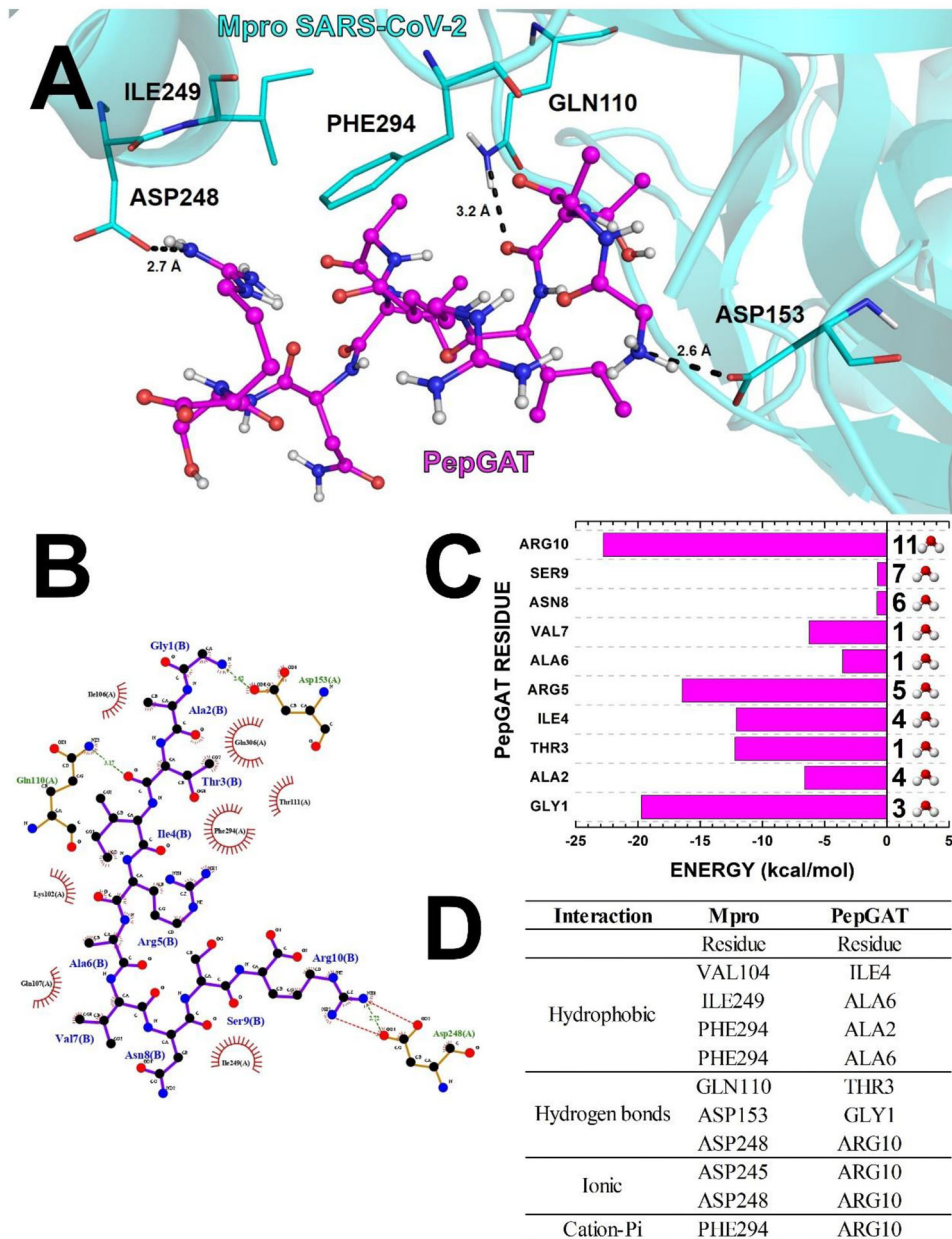


Figure 4. The 3D and 2D structure representations of the complex formed by docking of PepGAT (Gly¹-Ala-Thr-Ileu-Arg-Ala-Val-Asn-Ser-Arg¹⁰) on SARS-CoV-2 Mpro are depicted in A and B, respectively. The interaction energies of the amino acid residues of PepGAT with those of SARS-CoV-2 Mpro, and the amino acid residues that participate in the formation of hydrogen bond, hydrophobic, cation-pi, and ionic interactions between PepGAT and SARS-CoV-2 Mpro are shown in D.

is an RNA virus and has high mutational rates (Bzówka et al., 2020) and, for example, the antiviral 13b, which strongly binds to the proteolytic site of SARS-CoV-2 Mpro (Zhang et al., 2020), could quickly become ineffective against coronavirus. Prediction that *RcAlb*-PepII, PepGAT, and PepKAA interact with SARS-CoV-2 Mpro at a region far away from the protease active site (Figures 1, 8 and 9) is an advantage because besides their interactions being unaffected by mutation of the active site of SARS-CoV-2 Mpro, they induce conformational alterations in the 3D structure of this protease (Figure 8), as shown by the RMSD values of SARS-CoV-2 Mpro complexed with the peptides, compared to SARS-CoV-2 Mpro alone, that could disrupt the proteolytic activity of the viral enzyme, leading to a severe reduction in SARS-CoV-2

replication. Indeed, interaction of *RcAlb*-PepII, PepGAT, and PepKAA reduce the volume and area of SARS-CoV-2 Mpro proteolytic site, respectively, in 56.9% and 68.7% (Figure 9B), 38.4% and 36.0% (Figure 9C), and 23.1 and 13.0% (Figure 9D). In a recent report by our research group, it was shown that PepKAA also induced conformational changes in the SARS-CoV-2 Spike glycoprotein, disrupting its interaction with the ACE2 receptor located at the human cell membrane (Souza et al., 2020).

As PepKAA shows to interact with two different targets (SARS-CoV-2 Spike glycoprotein (Souza et al., 2020) and SARS-CoV-2 Mpro of SARS-CoV-2, this particular synthetic peptide is a potential small molecule candidate to be further tested *in vitro* against SARS-CoV-2, either alone or combined

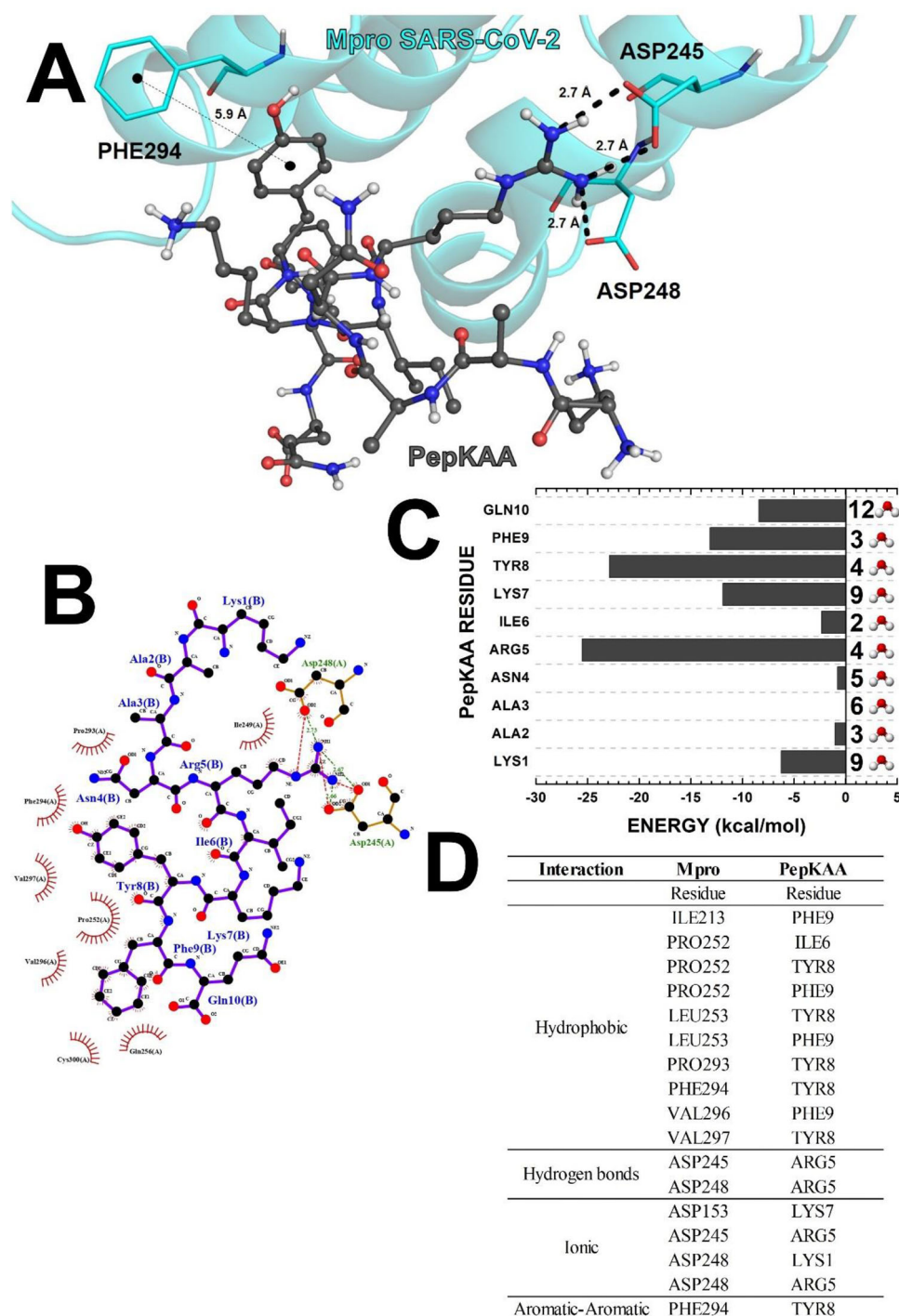


Figure 5. The 3D and 2D structure representations of the complex formed by docking of PepKAA (Lys¹-Ala-Ala-Asn-Arg-Ile-Lys-Tyr-Phe-Gln¹⁰) on SARS-CoV-2 Mpro are depicted in A and B, respectively. The interaction energies of the amino acid residues of PepKAA with those of SARS-CoV-2 Mpro, and the amino acid residues that participate in the formation of hydrogen bond, hydrophobic, ionic, and aromatic interactions between PepKAA and SARS-CoV-2 Mpro are shown in D.

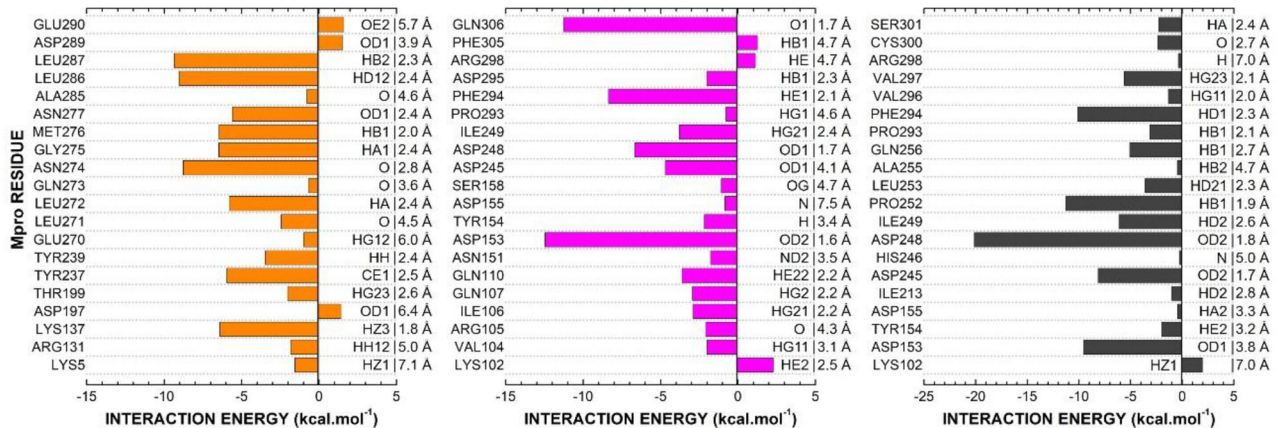
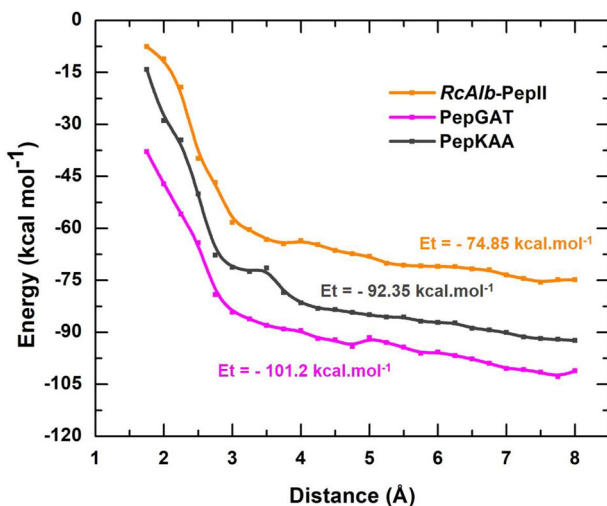
with other peptides like *RcAlb*-PepII, PepGAT. Of utmost importance is that *RcAlb*-PepII, PepGAT, and PepKAA were not toxic to mammalian cells like rabbit erythrocytes and human ABO type red blood cells (Dias et al., 2020; Oliveira et al., 2019; Souza et al., 2020), neither to fibroblast (lines L929 and MRC-5) and keratinocytes (Data not shown, manuscript in preparation).

5. Conclusion

Quantum biochemistry and molecular dynamics simulations allow to predicted that the peptides *RcAlb*-PepII, PepGAT, and PepKAA interact physically with SARS-CoV-2 Mpro and alter its 3D structure and provoke shrinkage of the active site of the protease. These findings suggest that these peptides

Table 4. Quantum parameters of the multi-point binding interactions between the amino acid residues of SARS-CoV-2 Mpro and those of PepKAA.

Amino acid residues				Residue charge		Residue atom	
SARS-CoV-2 Mpro	PepKAA	Distance (Å)	Free energy of interaction (kcal mol ⁻¹)	SARS-CoV-2 Mpro	PepKAA	SARS-CoV-2 Mpro	PepKAA
ASP245	ARG5	1.68	-11.93	-1	1	OD2	HH22
ASP248	ARG5	1.76	-11.32	-1	1	OD2	HH11
ASP248	LYS1	3.71	-10.36	-1	2	OD1	HB1
GLN256	PHE9	2.70	-6.55	0	0	HB1	HB1
PHE294	TYR8	2.31	-6.08	0	0	HD1	HE1
ASP153	LYS7	3.79	-4.93	-1	1	OD1	HZ3
ILE249	ARG5	2.60	-4.03	0	1	HD2	HD2
PRO252	TYR8	2.14	-3.60	0	0	HG1	HB1
VAL297	TYR8	2.14	-3.29	0	0	HG23	HA
ASP245	LYS1	7.09	-2.66	-1	2	OD1	HA
PRO252	ILE6	2.26	-2.60	0	0	HB2	HA
LEU253	PHE9	2.32	-2.50	0	0	HD21	HD2
TYR154	LYS7	3.17	-2.41	0	1	HE2	HE2
LEU253	TYR8	2.41	-2.40	0	0	HD22	HD2
PRO252	PHE9	1.90	-2.31	0	0	HB1	H
CYS300	PHE9	2.70	-1.77	0	0	O	HZ
ASP248	ALA2	4.12	-1.74	-1	0	OD2	H
PRO293	TYR8	2.06	-1.73	0	0	HB1	HE2
VAL247	ARG5	6.08	0.58	0	1	C	HH11
LYS102	LYS7	7.05	1.34	1	1	HZ1	HZ3

**Figure 6.** Binding site, interaction energy, and residue domain (BIRD) panel showing the MFCC interaction energies between the main amino acid residues of SARS-CoV-2 Mpro with those of *RcAlb*-PepII (A), PepGAT (B), and PepKAA (C). The minimal distance (Å) between each residue that participates in the interaction is indicated at the right side of the panel. The amino acid residues at the left side of the panel are from SARS-CoV-2 Mpro.**Figure 7.** Total interaction energy between SARS-CoV-2 Mpro and the Peptides as a function of the interaction distance. Orange, Magenta, and Black squares represent *RcAlb*-PepII, PepGAT, and PepKAA, respectively. Et accounts for the sum of the interaction energies up to 8 Å.

are likely antiviral small molecules that could potentially inhibit SARS-CoV-2 replication *in vivo*, a hypothesis that requires further investigation in the near future to be proven true. Importantly, besides to be apparently harmless to mammalian cells, *RcAlb*-PepII, PepGAT, and PepKAA do not interact with the active site of SARS-CoV-2 Mpro, unlike most antiviral drugs, and, thus, mutation of this protease domain will not affect the peptide effectiveness. In conclusion, this pioneering *in silico* investigation opens up opportunity for further *in vivo* investigations on these peptides, towards discovering new drugs and entirely new perspectives to treat COVID-19. For instance, peptide-based therapeutics have various advantages in relation to traditional small-molecule drugs, since peptides have higher specificity to selected targets, low toxicity because the possibility for accumulation in the body is improbable, and their synthesis is not a complex, costly, and time-consuming technique (VanPatten et al., 2020).

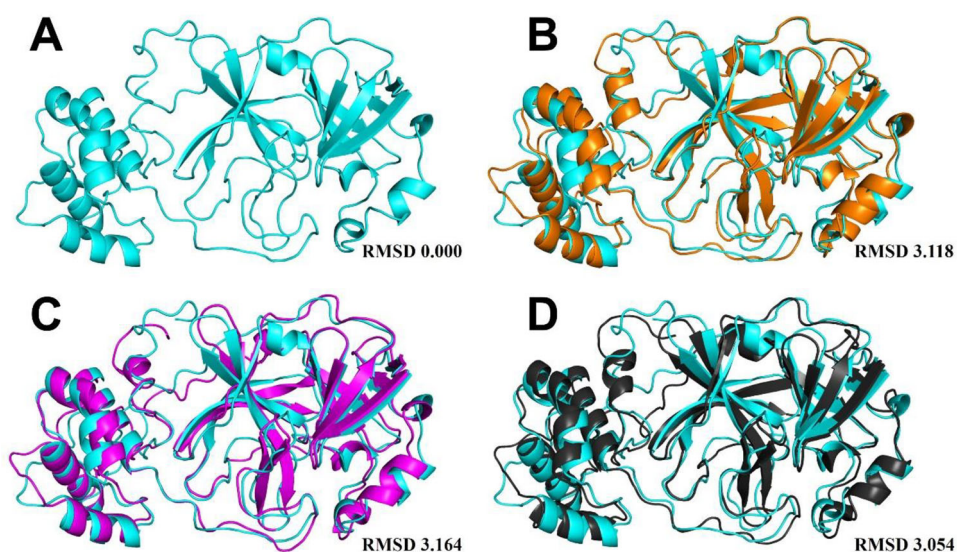


Figure 8. 3D visualization of the molecular complexes formed between SARS-CoV-2 Mpro and the peptides with the RMSD values of SARS-CoV-2 Mpro alone (in cyan, A) and when conjugated with *RcAlb*-PepII (B), PepGAT (C), and PepKAA (D). The merged structures suggest conformational alteration induced by the peptides.

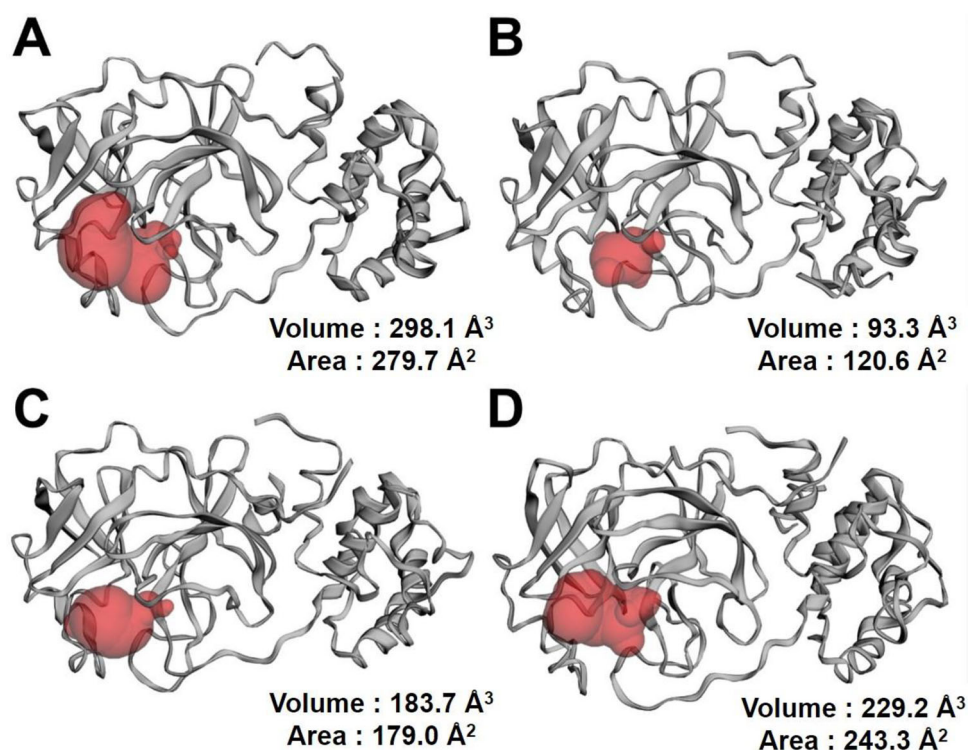


Figure 9. Conformational structure of the proteolytic site of SARS-CoV-2 Mpro alone and complexed with the peptides. The proteolytic site of SARS-CoV-2 Mpro alone (A) presents a volume and area higher than when SARS-CoV-2 Mpro is complexed with *RcAlb*-PepII (B), PepGAT (C), and PepKAA (D).

Acknowledgements

The authors are also grateful to the support received from the National Center for High Performance Processing - Federal University of Ceara and Center for Permanent Education in Health Care-CEATS/School of Public Health of Ceara (ESP-CE). V.N.F. also acknowledges support from PRONEX FUNCAP/CNPq (PR2-0101-00006.01.00/15).

Disclosure statement

No potential conflict of interest was reported by the authors.

Funding

This work was supported by grants from the following Brazilian agencies: The National Council for Scientific and Technological Development

(CNPq) with a doctoral grant to J.L.A. and research grant (codes 431511/2016-0 and 306202/2017-4) to J.T.A.O.; the Council for Advanced Professional Training (CAPES) sponsored PFNS with a Postdoctoral Fellowships.

Author contributions

Conceptualization: Pedro F. N. Souza, Jackson L. Amaral, Francisco E. S. Lopes, and Jose T. A. Oliveira. Data curation: Pedro F. N. Souza, Jackson L. Amaral, Francisco E. S. Lopes, Cleverson D. T. Freitas, and Valder N. Freire. Formal analysis: Pedro F. N. Souza, Jackson L. Amaral, and Francisco E. S. Lopes. Funding acquisition: Jose T. A. Oliveira, Cleverson D. T. Freitas, and Valder N. Freire. Methodology: Jackson L. Amaral and Francisco E. S. Lopes. Resources: Jose T. A. Oliveira, Cleverson D. T. Freitas, and Valder N. Freire. Supervision: Pedro F. N. Souza. Writing—original draft: Pedro F. N. Souza, Jackson L. Amaral, Francisco E. S. Lopes, and Leonardo V. Abreu. Writing—review and editing: Pedro F. N. Souza, Jackson L. Amaral, Francisco E. S. Lopes, Leonardo V. Abreu, and Jose T. A. Oliveira.

ORCID

Jackson L. Amaral  <http://orcid.org/0000-0002-8745-1247>

Pedro F. N. Souza  <http://orcid.org/0000-0003-2524-4434>

Reference

- Almazán, F., Sola, I., Zuñiga, S., Marquez-Jurado, S., Morales, L., Becares, M., & Enjuanes, L. (2014). Coronavirus reverse genetic systems: Infectious clones and replicons. *Virus Research*, *189*, 262–270. <https://doi.org/10.1016/j.virusres.2014.05.026>
- Amaral, J. L., Santos, S. J. M., Souza, P. F. N., de Moraes, P. A., Maia, F. F., Carvalho, H. F., & Freire, V. N. (2020). Quantum biochemistry in cancer immunotherapy: New insights about CTLA-4/ipilimumab and design of ipilimumab-derived peptides with high potential in cancer treatment. *Molecular Immunology*, *127*, 203–211. <https://doi.org/10.1016/j.molimm.2020.09.013>
- Bzówka, M., Mitusińska, K., Raczyńska, A., Samol, A., Tuszyński, J. A., & Góra, A. (2020). Structural and evolutionary analysis indicate that the SARS-CoV-2 Mpro is a challenging target for small-molecule inhibitor design. *International Journal of Molecular Sciences*, *21*(9), 3099. <https://doi.org/10.3390/ijms21093099>
- Campos, D. M. O., Bezerra, K. S., Esmail, S. C., Fulco, U. L., Albuquerque, E. L., & Oliveira, J. I. N. (2020). Intermolecular interactions of cn-716 and acyl-KR-aldehyde dipeptide inhibitors against Zika virus. *Physical Chemistry Chemical Physics*, *22*(27), 15683–15695. <https://doi.org/10.1039/D0CP02254C>
- CDC. (n.d). COVIDView: A weekly surveillance summary of U.S. COVID-19 activity. <https://www.cdc.gov/coronavirus/2019-ncov/covid-data/covid-view/index.html>
- Dai, W., Zhang, B., Jiang, X. M., Su, H., Li, J., Zhao, Y., Xie, X., Jin, Z., Peng, J., Liu, F., Li, C., Li, Y., Bai, F., Wang, H., Cheng, X., Cen, X., Hu, S., Yang, X., Wang, J., ... Liu, H. (2020). Structure-based design of antiviral drug candidates targeting the SARS-CoV-2 main protease. *Science*, *368*(6497), 1331–1335. <https://doi.org/10.1126/science.abb4489>
- Delley, B. (2000). From molecules to solids with the DMol3 approach. *Journal of Chemical Physics*, *113*(18), 7756–7764. <https://doi.org/10.1063/1.1316015>
- Diamond, M. S., & Pierson, T. C. (2020). The challenges of vaccine development against a new virus during a pandemic. *Cell Host & Microbe*, *27*(5), 699–703. <https://doi.org/10.1016/j.chom.2020.04.021>
- Dias, L. P., Souza, P. F. N., Oliveira, J. T. A., Vasconcelos, I. M., Araújo, N. M. S., Tilburg, M. F. V., Guedes, M. I. F., Carneiro, R. F., Lopes, J. L. S., & Sousa, D. O. B. (2020). RAlb-PeplI, a synthetic small peptide bioinspired in the 2S albumin from the seed cake of *Ricinus communis*, is a potent antimicrobial agent against *Klebsiella pneumoniae* and *Candida parapsilosis*. *Biochimica et Biophysica Acta (Bba) - Biomembranes*, *1862*(2), 183092. <https://doi.org/10.1016/j.bbamem.2019.183092>
- Estrada, E. (2020). Topological analysis of SARS CoV-2 main protease. *Chaos: An Interdisciplinary Journal of Nonlinear Science*, *30*(6), 061102. <https://doi.org/10.1063/5.0013029>
- Hall, D. C., & Ji, H.-F. (2020). A search for medications to treat COVID-19 via in silico molecular docking models of the SARS-CoV-2 spike glycoprotein and 3CL protease. *Travel Medicine and Infectious Disease*, *35*, 101646. <https://doi.org/10.1016/j.tmaid.2020.101646>
- Hoffmann, M., Kleine-Weber, H., Schroeder, S., Krüger, N., Herrler, T., Erichsen, S., Schiergens, T. S., Herrler, G., Wu, N. H., Nitsche, A., Müller, M. A., Drosten, C., & Pöhlmann, S. (2020). SARS-CoV-2 cell entry depends on ACE2 and TMPRSS2 and is blocked by a clinically proven protease inhibitor. *Cell*, *181*(2), 271–280.e8. <https://doi.org/10.1016/j.cell.2020.02.052>
- Hui, D. S., I Azhar, E., Madani, T. A., Ntoumi, F., Kock, R., Dar, O., Ippolito, G., Mchugh, T. D., Memish, Z. A., Drosten, C., Zumla, A., & Petersen, E. (2020). The continuing 2019-nCoV epidemic threat of novel coronaviruses to global health — The latest 2019 novel coronavirus outbreak in Wuhan, China. *International Journal of Infectious Diseases*, *91*, 264–266. <https://doi.org/10.1016/j.ijid.2020.01.009>
- Laskowski, R. A., & Swindells, M. B. (2011). LigPlot+: Multiple ligand-protein interaction diagrams for drug discovery. *Journal of Chemical Information and Modeling*, *51*(10), 2778–2786. <https://doi.org/10.1021/ci200227u>
- Laskowski, R. A., Jabłońska, J., Pravda, L., Vařeková, R. S., & Thornton, J. M. (2018). PDBsum: Structural summaries of PDB entries. *Protein Science*, *27*(1), 129–134. <https://doi.org/10.1002/pro.3289>
- Li, H., Liu, L., Zhang, D., Xu, J., Dai, H., Tang, N., Su, X., & Cao, B. (2020). SARS-CoV-2 and viral sepsis: Observations and hypotheses. *Lancet*, *395*(10235), 1517–1520. [https://doi.org/10.1016/S0140-6736\(20\)30920-X](https://doi.org/10.1016/S0140-6736(20)30920-X)
- Liu, S., Zheng, Q., & Wang, Z. (2020). Potential covalent drugs targeting the main protease of the SARS-CoV-2 coronavirus. *Bioinformatics*, *36*(11), 3295–3298. <https://doi.org/10.1093/bioinformatics/btaa224>
- Moal, I. H., & Bates, P. A. (2010). SwarmDock and the use of normal modes in protein-protein Docking. *International Journal of Molecular Sciences*, *11*(10), 3623–3648. <https://doi.org/10.3390/ijms11103623>
- Moraes, P. A., Maia, F. F., Solis-Calero, C., Caetano, E. W. S., Freire, V. N., & Carvalho, H. F. (2020). The urokinase plasminogen activator binding to its receptor: A quantum biochemistry description within an in/homogeneous dielectric function framework with application to uPA-uPAR peptide inhibitors. *Physical Chemistry Chemical Physics*, *22*(6), 3570–3583. <https://doi.org/10.1039/C9CP06530J>
- Ngo, S. T., Quynh Anh Pham, N., Thi Le, L., Pham, D.-H., & Vu, V. V. (2020). Computational determination of potential inhibitors of SARS-CoV-2 main protease. *Journal of Chemical Information and Modeling*, *60*(12), 5771–5780. <https://doi.org/10.1021/acs.jcim.0c00491>
- Oliveira, J. T. A., Souza, P. F. N., Vasconcelos, I. M., Dias, L. P., Martins, T. F., Van Tilburg, M. F., Guedes, M. I. F., & Sousa, D. O. B. (2019). Mo-CBP3-PeplI, Mo-CBP3-PeplII, and Mo-CBP3-PeplIII are synthetic antimicrobial peptides active against human pathogens by stimulating ROS generation and increasing plasma membrane permeability. *Biochimie*, *157*, 10–21. <https://doi.org/10.1016/j.biochi.2018.10.016>
- Ortega, J. T., Serrano, M. L., Pujol, F. H., & Rangel, H. R. (2020). Unrevealing sequence and structural features of novel coronavirus using in silico approaches: The main protease as molecular target. *EXCLI J*, *19*, 400–409. <https://doi.org/10.17179/excli2020-1189>
- Practice, B. M. J. B. (2020). Coronavirus disease 2019. *World Health Organization*, *2019*, 2633. <https://doi.org/10.1001/jama.2020.2633>
- Ragab, D., Salah Eldin, H., Taeimah, M., Khattab, R., & Salem, R. (2020). The COVID-19 cytokine storm; what we know so far. *Frontiers in Immunology*, *11*, 1446. <https://doi.org/10.3389/fimmu.2020.01446>
- Ramírez-Aportela, E., Ramón López-Blanco, J., & Chacón, P. (2016). Structural bioinformatics FRODOCK 2.0: Fast protein-protein docking server, 2008–2010. <http://frodock.chaconlab.org>

- Robertson, M. J., Tirado-Rives, J., & Jorgensen, W. L. (2015). Improved peptide and protein torsional energetics with the OPLS-AA force field. *Journal of Chemical Theory and Computation*, 11(7), 3499–3509. <https://doi.org/10.1021/acs.jctc.5b00356>
- Saxena, A. (2020). Drug targets for COVID-19 therapeutics: Ongoing global efforts. *Journal of Biosciences*, 45(1), 87. <https://doi.org/10.1007/s12038-020-00067-w>
- Serafin, M. B., Bottega, A., Foletto, V. S., da Rosa, T. F., Hörner, A., & Hörner, R. (2020). Drug repositioning is an alternative for the treatment of coronavirus COVID-19. *International Journal of Antimicrobial Agents*, 55(6), 105969. <https://doi.org/10.1016/j.ijantimicag.2020.105969>
- Sharma, P., Vijayan, V., Pant, P., Sharma, M., Vikram, N., Kaur, P., Singh, T. P., & Sharma, S. (2020). Identification of potential drug candidates to combat COVID-19: A structural study using the main protease (mpro) of SARS-CoV-2. *Journal of Biomolecular Structure and Dynamics*, 0, 1–11. <https://doi.org/10.1080/07391102.2020.1798286>
- Song, Z., Xu, Y., Bao, L., Zhang, L., Yu, P., Qu, Y., Zhu, H., Zhao, W., Han, Y., & Qin, C. (2019). From SARS to MERS, thrusting coronaviruses into the spotlight. *Viruses*, 11(1), 59. <https://doi.org/10.3390/v11010059>
- Sousa, B. L., Barroso-Neto, I. L., Oliveira, E. F., Fonseca, E., Lima-Neto, P., Ladeira, L. O., & Freire, V. N. (2016). Explaining RANKL inhibition by OPG through quantum biochemistry computations and insights into peptide-design for the treatment of osteoporosis. *RSC Advances*, 6(88), 84926–84942. <https://doi.org/10.1039/C6RA16712H>
- Souza, P. F. N., Lopes, F. E. S., Amaral, J. L., Freitas, C. D. T., & Oliveira, J. T. A. (2020). A molecular docking study revealed that synthetic peptides induced conformational changes in the structure of SARS-CoV-2 spike glycoprotein, disrupting the interaction with human ACE2 receptor. *International Journal of Biological Macromolecules*, 164, 66–76. <https://doi.org/10.1016/j.ijbiomac.2020.07.174>
- Souza, P. F. N., Marques, L. S. M., Oliveira, J. T. A., Lima, P. G., Dias, L. P., Neto, N. A. S., Lopes, F. E. S., Sousa, J. S., Silva, A. F. B., Caneiro, R. F., Lopes, J. L. S., Ramos, M. V., & Freitas, C. D. T. (2020). Synthetic antimicrobial peptides: From choice of the best sequences to action mechanisms. *Biochimie*, 175, 132–145. <https://doi.org/10.1016/j.biochi.2020.05.016>
- Souza, P. F. N., Mesquita, F. P., Amaral, J. L., Lima P. G. C., Lima K. R. P., Costa, M. B., Farias, I. R., Lima, L. B., & Montenegro, R. C. (2021). The Human Pandemic Coronaviruses on the Show: The Spike Glycoprotein as the Main Actor in the Coronaviruses Play. *International Journal of Biological Macromolecules*, 179, 1–19. <https://doi.org/10.1016/j.ijbiomac.2021.02.203>
- Tang, Y., Liu, J., Zhang, D., Xu, Z., Ji, J., & Wen, C. (2020). Cytokine storm in COVID-19: The current evidence and treatment strategies. *Frontiers in Immunology*, 11, 1708. <https://doi.org/10.3389/fimmu.2020.01708>
- Tay, M. Z., Poh, C. M., Rénia, L., MacAry, P. A., & Ng, L. F. P. (2020). The trinity of COVID-19: Immunity, inflammation and intervention. *Nature Reviews Immunology*, 20(6), 363–374. <https://doi.org/10.1038/s41577-020-0311-8>
- Tian, W., Chen, C., Lei, X., Zhao, J., & Liang, J. (2018). CASTp 3.0: Computed atlas of surface topography of proteins. *Nucleic Acids Research*, 46(W1), W363–W367. <https://doi.org/10.1093/nar/gky473>
- Van Der Spoel, D., Lindahl, E., Hess, B., Groenhof, G., Mark, A. E., & Berendsen, H. J. C. (2005). GROMACS: Fast, flexible, and free. *Journal of Computational Chemistry*, 26(16), 1701–1718. <https://doi.org/10.1002/jcc.20291>
- VanPatten, S., He, M., Altit, A., Cheng, K. F., Ghanem, M. H., & Al-Abed, Y. (2020). Evidence supporting the use of peptides and peptidomimetics as potential SARS-CoV-2 (COVID-19) therapeutics. *Future Medicinal Chemistry*, 12(18), 1647–1656.
- WHO. (2020). *Middle East respiratory syndrome coronavirus (MERS-CoV)*. WHO.
- Wu, A., Peng, Y., Huang, B., Ding, X., Wang, X., Niu, P., Meng, J., Zhu, Z., Zhang, Z., Wang, J., Sheng, J., Quan, L., Xia, Z., Tan, W., Cheng, G., & Jiang, T. (2020). Genome composition and divergence of the novel coronavirus (2019-nCoV) originating in China. *Cell Host & Microbe*, 27(3), 325–328. <https://doi.org/10.1016/j.chom.2020.02.001>
- Yuan, Y., Cao, D., Zhang, Y., Ma, J., Qi, J., Wang, Q., Lu, G., Wu, Y., Yan, J., Shi, Y., Zhang, X., & Gao, G. F. (2017). Cryo-EM structures of MERS-CoV and SARS-CoV spike glycoproteins reveal the dynamic receptor binding domains. *Nature Communications*, 8, 15092. <https://doi.org/10.1038/ncomms15092>
- Zhang, D. W., & Zhang, J. Z. H. (2003). Molecular fractionation with conjugate caps for full quantum mechanical calculation of protein-molecule interaction energy. *Journal of Chemical Physics*, 119(7), 3599–3605. <https://doi.org/10.1063/1.1591727>
- Zhang, L., Lin, D., Sun, X., Curth, U., Drosten, C., Sauerhering, L., Becker, S., Rox, K., & Hilgenfeld, R. (2020). Crystal structure of SARS-CoV-2 main protease provides a basis for design of improved a-ketoamide inhibitors. *Science*, 368(6489), 409–412. <https://doi.org/10.1126/science.abb3405>
- Zhang, Y., Xu, J., Jia, R., Yi, C., Gu, W., Liu, P., Dong, X., Zhou, H., Shang, B., Cheng, S., Sun, X., Ye, J., Li, X., Zhang, J., Ling, Z., Ma, L., Wu, B., Zeng, M., Zhou, W., & Sun, B. (2020). Protective humoral immunity in SARS-CoV-2 infected pediatric patients. *Cellular and Molecular Immunology*, 17, 768–770. <https://doi.org/10.1038/s41423-020-0438-3>
- Ziebuhr, J., Snijder, E. J., & Gorbalenya, A. E. (2000). Virus-encoded proteinases and proteolytic processing in the Nidovirales. *Journal of General Virology*, 81(4), 853–879. <https://doi.org/10.1099/0022-1317-81-4-853>